异质接头应力集中系数与坡口角度和材料差异度的关系方程

薛 钢[1,2]， 王 涛[2]， 方洪渊[1]
(1. 哈尔滨工业大学 先进焊接与连接国家重点实验室，哈尔滨 150001;
2. 中国船舶重工集团公司 第七二五研究所，洛阳 471023)

摘 要：基于有限单元法针对异质对接接头设计，以提高接头疲劳承载能力以及更准确的预测异质接头疲劳失效位置为目标，考察了坡口角度和材料差异度对异质对接接头焊趾应力集中系数和焊根应力集中系数的影响，并给出了削平异质对接接头焊趾和焊根应力集中系数与坡口角度和材料差异度之间的关系方程. 结果表明，随着坡口角度和材料差异度的增加，对接接头焊根应力集中系数增大，焊趾应力集中系数减小. 应力集中系数关系方程与有限元结果吻合较好，相对误差在3%以内.

关键词：焊根应力集中系数；焊趾应力集中系数；坡口角度；材料差异度
中图分类号：TG 405 **文献标识码**：A **文章编号**：0253－360X(2014)08－0095－04

0 序 言

疲劳是引起工程构件尤其是船体结构失效的主要原因，其中焊接接头由于应力集中、残余应力、焊接缺欠和材质性能差等因素而成为主要的疲劳发生部位，而接头的应力集中是影响接头疲劳性能的重要因素，需要予以重点关注[1－3].

为节约材料、减轻结构重量、降低建造成本，提高强度是结构钢一直以来的发展趋势，尤其对于船体结构用钢，各国都在不断发展高强度新钢种[4]. 但是随着结构钢强度的提高，焊接冷裂纹产生倾向也不断增大[5,6]. 为避免焊接冷裂纹的产生，除采用热输入控制、焊前预热、焊后保温等工艺措施外，还可通过开发对冷裂纹不敏感、强度低于母材的配套奥氏体焊接材料. 而对于采用奥氏体焊材焊接形成的“F-A-F”(“铁素体－奥氏体－铁素体”)异种材质焊接接头，母材和焊缝金属在晶体结构特性(晶体类型、滑移系、柏氏矢量)和相变特性上存在显著差别，导致两者在微观塑性变形能力和宏观力学性能(杨氏模量、屈服应力、形变硬化能力、循环软硬化特性)存在差异并形成明显的界面，引起承载条件下接头各部位的变形不协调[7,8]. 另外焊接坡口角度也会对异质焊接接头应力集中产生影响. 然而针对异质焊接接头的坡口角度和材料差异度对接头应力集中系数的影响一直未有研究.

文中通过对不同坡口角度和材料差异度异质对接接头应力集中系数的有限元计算，明确了异质接头焊根和焊趾应力集中系数与坡口角度和材料差异度之间的关系，为异质接头的疲劳失效位置预测以及疲劳性能评价提供了重要技术支撑.

1 基本概念

文中研究对象为X形坡口的削平异质对接接头，由于接头的对称性，其1/2结构如图1所示，其中α为坡口角度的一半. 此时考虑接头材料的差异度为焊缝金属和母材金属的杨氏模量差异.

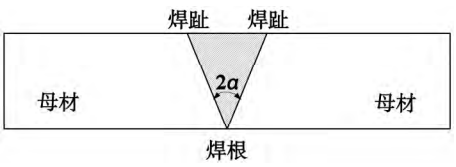

图1 X形坡口的1/2异质对接接头
Fig. 1 1/2 heterogeneous butt joint with X-groove

焊根应力集中系数是指焊根处峰值应力与远端母材所承受的平均应力的比值，焊趾应力集中系数是指焊趾应力与远端母材所承受的平均应力的比值. 此时接头处的峰值应力应小于焊缝金属的屈服强度.

收稿日期：2014－01－28

2 有限元模型的建立

考虑到接头的对称性，取 1/4 接头进行有限元分析，图 2 为板厚 16 mm，α 为 30°的异质对接接头有限元模型. 模型采用平面应变四边形四节点单元，为保证结果的准确性，焊趾和焊根附近网格尽量细化，最小网格尺寸为 0.02 mm. 为方便分析，以下计算都以母材厚度 16 mm 为例. 图 3 为板厚 16 mm，α 为 30°，焊缝和母材金属杨氏模量比值为 0.5 的异质对接接头承受 100 MPa 外加应力时的应变云图. 从应变云图可知，异质接头焊缝金属和母材金属的应变存在较大差异，尤其是焊根处产生明显的应变集中，这将导致焊根处的应力集中.

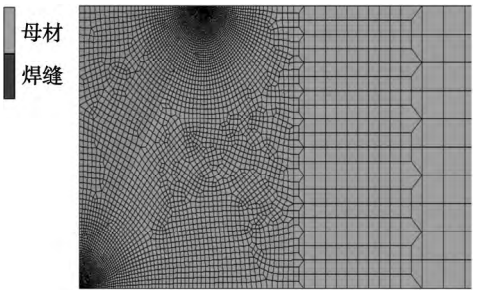

图 2 1/4 异质接头有限元模型

Fig. 2 1/4 FEA model of heterogeneous butt joint

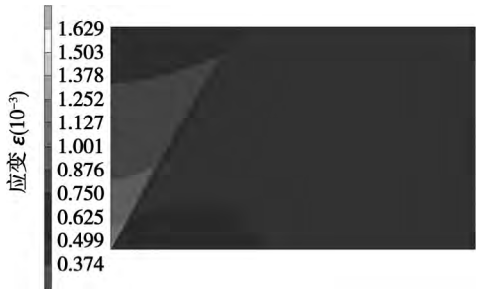

图 3 焊缝与母材杨氏模量比为 0.5 且 α 为 30°时接头应变云图

Fig. 3 Thestrain contour of butt joint with 30°half of groove angle and 0.5 E ratio of weld to base metal

3 计算结果及分析

为研究材料差异度和坡口角度对接头应力集中系数的影响，研究材料差异度对应力集中系数影响时，固定坡口角度，每个材料差异度对应一组焊趾应力集中系数和焊根应力集中系数. 同理，研究坡口角度对应力集中系数影响时，固定材料差异度，每个坡口角度对应一组焊趾应力集中系数和焊根应力集中系数. 为方便分析，以 16 mm 板厚为例研究坡口角度和材料差异度对异质接头应力集中系数的影响.

图 4 和图 5 分别为焊缝和母材金属杨氏模量 E 比值在 0.5 ~ 1.0 范围变化时，坡口角度对异质对接接头焊根应力集中系数和焊趾应力集中系数的影响. 结果表明，对于异质接头而言，当焊缝金属的杨氏模量小于母材金属的杨氏模量时，随着坡口角度的增大，对接接头焊根应力集中系数增大，焊趾应力集中系数减小. 焊缝金属与母材金属的杨氏模量差异度越大，坡口角度对焊根和焊趾应力集中系数的影响程度越大. 异质接头焊根处的应力集中系数均大于 1，焊趾处的应力集中系数均小于 1. 这是由于焊趾位于接头上下表面母材金属和焊缝金属分界处，坡口角度越大，从焊缝中心到焊趾处的“软质”焊缝金属越多，承受相同外加载荷时，接头表面的焊缝金属协调变形越充分，焊趾处(焊缝金属)的应力和应变越小，焊趾处的应力集中系数越小. 坡口角度越大时，接头上下表面附近的焊缝中心金属的变形协调越充分，应力和应变越小且趋于稳定，由于接头厚度方向焊缝中心金属的平均应力和应变一定，

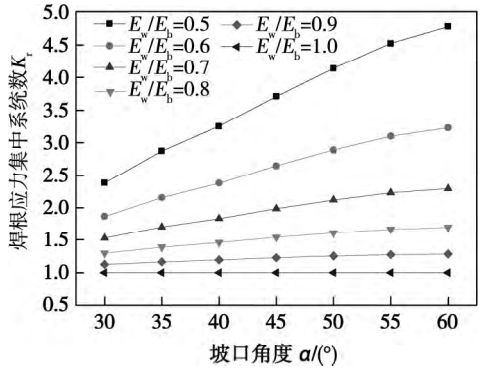

图 4 坡口角度对焊根应力集中系数的影响

Fig. 4 Influence of groove angle on weld root stress concentration factor of heterogeneous butt joint

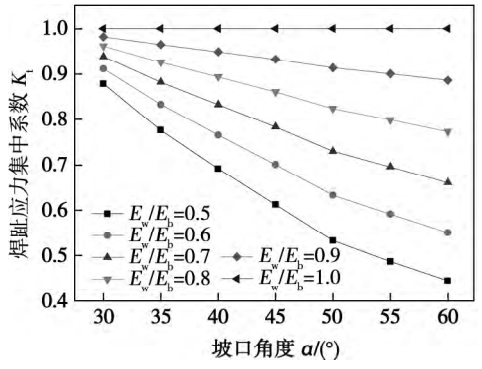

图 5 坡口角度对焊趾应力集中系数的影响曲线

Fig. 5 Influence of groove angle on weld toe stress concentration factor of heterogeneous butt joint

导致焊根处的应力集中系数越大.

图 6 和图 7 分别为 α 在 30° ~ 60°范围变化时,焊缝和母材金属杨氏模量比值对异质对接接头焊根应力集中系数和焊趾应力集中系数的影响. 结果表明,对于异质接头而言,当坡口角度一定时,随着焊缝金属母材金属的杨氏模量比值的减小(材料差异度越大),对接接头焊根应力集中系数增大,焊趾应力集中系数减小. 坡口角度越大,焊缝金属与母材金属的杨氏模量差异度对焊根和焊趾应力集中系数的影响程度越大. 这是由于接头材料差异度越大,焊缝和母材金属部位的变形越不协调,焊根和焊趾处的应力集中程度越严重. 由于成分系的不同,目前奥氏体钢熔敷金属的弹性模量范围为 150 ~ 190 GPa,铁素体钢的弹性模量为 210 GPa 左右,因此"F-A-F"异种接头焊缝金属和母材金属的杨氏模量比值范围大致为 0.7 ~ 0.9. 以 α 为 30°的情况为例,接头焊缝金属和母材金属的杨氏模量比值为 0.7 和 0.9 时,对应的焊根应力集中系数分别为 1.527 和 1.127,差异 35.5%. 接头焊缝金属和母材金属的杨氏模量比值为 0.7 和 0.9 时,对应的焊趾应力集中系数分别为 0.939 和 0.982,差异 4.4%.

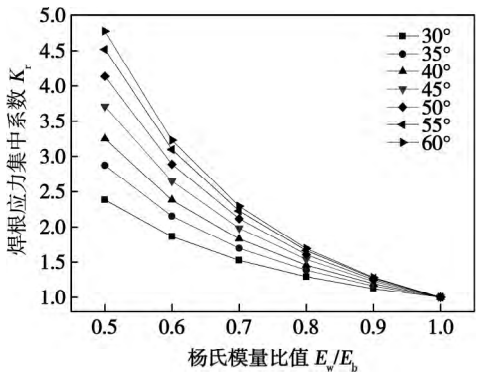

图 6　焊根应力集中系数与材料杨氏模量比值的关系曲线

Fig. 6　Influence of Young's modulus ratio on weld root stress concentration factor of heterogeneous butt joint

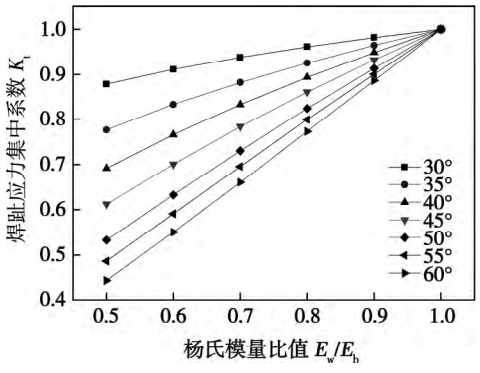

图 7　焊趾应力集中系数与材料杨氏模量比值的关系曲线

Fig. 7　Influence of Young's modulus ratio on weld toe stress concentration factor of heterogeneous butt joint

4　应力集中系数关系方程

4.1　焊根应力集中系数关系方程

根据以上焊根应力集中系数与坡口角度和焊接材料差异度关系曲线的变化趋势,将焊根应力集中系数计算结果对焊缝与母材金属杨氏模量比值进行回归分析,得到焊根应力集中系数关系方程为

$$K_r = A_1 + B_1 \exp\left[-C_1 \left(\frac{E_w}{E_b} - 1 \right) \right] \tag{1}$$

式中: K_r 为焊根应力集中系数; E_w 为焊缝金属杨氏模量; E_b 为母材金属杨氏模量; A_1, B_1, C_1 为与坡口角度有关的系数.

$$A_1 = 0.552\,7 + 1.096\,1\exp(-2.883\,9\tan\alpha) \tag{2}$$

$$B_1 = 0.468\,2 - 1.120\,4\exp(-2.817\,4\tan\alpha) \tag{3}$$

$$C_1 = 4.987\,1 - 1.884\,3\exp(-0.731\,6\tan\alpha) \tag{4}$$

4.2　焊趾应力集中系数关系方程

根据以上焊趾应力集中系数与坡口角度和焊接材料差异度关系曲线的变化趋势,将焊趾应力集中系数计算结果对焊缝与母材金属杨氏模量比值进行回归分析,得到焊趾应力集中系数关系方程为

$$K_t = A_2 + B_2 \frac{E_w}{E_b} \tag{5}$$

式中: K_t 为焊趾应力集中系数; A_2, B_2 为与坡口角度有关的系数.

$$A_2 = -0.244\,8 + 2.870\,8\exp(-1.806\,6\tan\alpha) \tag{6}$$

$$B_2 = 1.230\,2 - 2.931\,9\exp(-1.877\,9\tan\alpha) \tag{7}$$

按式(1)和式(5)分别计算不同坡口角度和材料差异度时削平异质对接接头的焊根应力集中系数和焊趾应力集中系数,与有限元计算结果相比,误差均在 3% 以内.

根据应力集中系数关系方程,可以计算某一坡口角度和材料差异度时接头的焊根和焊趾应力集中系数,反之当坡口角度或材料差异度确定时,可以得到特定应力集中系数下对应的材料差异度或坡口角度,应力集中系数关系方程对于削平异质对接接头的设计具有指导意义.

以上应力集中系数方程未考虑钝边尺寸、板厚、余高形状以及焊接残余应力等因素的影响,文中仅从坡口角度和材料差异度角度考虑了接头应力集中系数的变化规律. 在以后的研究中,应完善不同因

素对接头应力集中系数的影响.

5 结 论

(1) 当焊缝金属的杨氏模量小于母材金属的杨氏模量时,随着坡口角度的增加,对接接头焊根应力集中系数增大,焊趾应力集中系数减小. 焊缝金属与母材金属的杨氏模量差异度越大,坡口角度对焊根和焊趾应力集中系数的影响程度越大.

(2) 当坡口角度一定时,随着焊缝金属与母材金属的杨氏模量比值的减小,对接接头焊根应力集中系数增大,焊趾应力集中系数减小. 坡口角度越大,焊缝金属与母材金属的杨氏模量差异度对焊根和焊趾应力集中系数的影响程度越大.

参考文献:

[1] 王佳杰,杨建国,方洪渊. 随焊冲击碾压整形新方法及等承载接头拉伸与疲劳性能[J]. 焊接学报,2012,33(11):35-38.
Wang Jiajie, Yang Jianguo, Fang Hongyuan. A new weld shaping method with trailing impact rolling and tensile and fatigue properties for equal load-carrying capacity joints [J]. Transactions of the China Welding Institution, 2012, 33 (11): 35-38.

[2] 闫忠杰,方洪渊,刘雪松. 机械整形新技术对铝合金焊接接头疲劳性能的影响[J]. 焊接学报,2013,34(7):81-84.
Yan Zhongjie, Fang Hongyuan, Liu Xuesong. Eeffect of mechanical shaping method on fatigue property of aluminium alloy welded joint [J]. Transactions of the China Welding Institution, 2013, 34 (7): 81-84.

[3] 赵东升,吴国强. 焊接残余应力对 Invar 钢疲劳寿命影响分析[J]. 焊接学报,2013,34(4):93-95.
Zhao Dongsheng, Wu Guoqiang. Effect of welding residual stress on fatigue life of Invar steel welded jiont [J]. Transactions of the China Welding Institution, 2013, 34(4): 93-95.

[4] Helen Zhang, David Jin. Study states on surface protection of DS surface material damage [J]. Advanced Materials Research, 2012, 531: 168-172.

[5] 张元杰,彭 云,马成勇. Q890 高强钢焊接淬硬倾向和冷裂纹敏感性[J]. 焊接学报,2013,34(6):53-56.
Zhang Yuanjie, Peng Yun, Ma Chengyong. Harden quenching tendency and cold cracking susceptibility of Q890 steel during welding [J]. Transactions of the China Welding Institution, 2013, 34(6): 53-56.

[6] 陶世森,宗 培,董积旖. 环肋圆柱壳的肋骨环焊缝焊接拘束度计算方法[J]. 焊接学报,2013,34(8):97-100.
Tao Shisen, Zong Pei, Dong Jiyi. The calculation method for welding restraint intensity of fillet weld in ring-stiffened cylinder [J]. Transactions of the China Welding Institution, 2013, 34(8): 97-100.

[7] 杨建国,陈双建,苑世剑. 304 不锈钢形变诱导马氏体相变的影响因素分析[J]. 焊接学报,2012,33 (12): 89-92.
Yang Jianguo, Chen Shuangjian, Yuan Shijian. Factors affecting deformation induced martensitic transformation of SUS304 stainless steel [J]. Transactions of the China Welding Institution, 2012, 33 (12): 89-92.

[8] William D, Callister. Materials science and engineering (7th edition) [M]. USA: John Wiley & Sons, Inc, 2007.

作者简介: 薛 钢,男,1978 年出生,博士. 主要从事焊接结构安全可靠性的研究工作. 发表论文 10 余篇. Email: xuegang_29@163.com

通讯作者: 方洪渊,男,博士研究生导师,教授. Email: hyfang@hit.edu.cn

fabrication.

Key words: SA738Gr. B steel; thermal simulation; heat affected zone; mechanical property

Stress concentration factor equation of heterogeneity joint based on slope angle and material difference XUE Gang[1,2], WANG Tao[2], FANG Hongyuan[1] (1. State Key Laboratory of Advanced Welding and Joining, Harbin Institute of Technology, Harbin 150001, China; 2. Luoyang Ship Material Research Institute, Luoyang 471023, China). pp 95 – 98

Abstract: In order to improve the fatigue load carrying capacity and efficiently predict the fatigue failure position of heterogeneous joint, the influences of groove angle and difference between welded materials on joint stress concentration factor are studied based on finite element method. The weld root stress concentration factor and weld toe stress concentration factor relation equations of flat heterogeneous butt joint are also developed. The result shows that weld root stress concentration factor increases with the increase of groove angle and difference between welded materials, weld toe stress concentration factor decreases with the increase of groove angle and difference between welded materials. The results calculated by stress concentration factor relation equations are in good agreement with the finite element method results, and the relative error is less than 3%.

Key words: weld root stress concentration factor; weld toe stress concentration factor; groove angle; difference between welded materials

Analysis and evaluation of arc stability of self-shielded flux-cored wire in all-position welding ZHANG Tianli[1], LI Zhuoxin[2], JING Hongyang[1], LI Guodong[2], LI Hong[2], SONG Shaopeng[2] (1. School of Materials Science and Engineering, Tianjin University, Tianjin 300072, China; 2. College of Materials Science and Engineering, Beijing University of Technology, Beijing 100124, China). pp 99 – 102

Abstract: The droplet transfer and arc stability of three kinds of self-shielded flux-cored wires in all-position welding applied in X70 pipeline steel were tested by using high-speed video camera and Hanover Analysator. The results showed that as for all-position welding arc stability, No. 1 wire was the best, No. 3 wire the medium, and No. 2 wire the worst; coefficient of current variability could reflect welding stability more accurately than standard deviation; average short-circuiting time could not be taken as the only way to judge welding arc stability, which should be judged by combining with class frequency distributions diagram of short-circuiting time. During short circuiting transfer, probability density distributions diagram of arc voltage was in double-hump shape, and probability density distributions of double-hump shape curve and convergence of the whole curve could be regarded as important references for evaluating welding arc stability.

Key words: self-shielded flux cored wire; all-position welding; droplet transfer; welding arc stability

Microstructure and properties of simulated heat affected zones of weathering heavy steel plate for bridge CHENG Binggui, LIU Dongsheng (Institute of Research of Iron and Steel (IRIS), Shasteel, Zhangjiagang 215625, China). pp 103 – 107, 112

Abstract: Advanced heavy steel plates (60 mm thick) for bridge with room temperature yield-strength greater than 500 MPa and assured low temperature impact toughness (Charpy V notch impact energy (CVN) of 200 J at -40 ℃) have been produced via thermomechanical control process (TMCP). The dependence of microstructure and the impact toughness at -40 ℃ of the coarse-grained heat-affected zone (CGHAZ) generated by single-pass simulated welding upon the heat input energy (E) and peak temperature T_P^2 of simulated second-pass welding processes were revealed. Thermal cycles of the CGHAZ and the sub-regions (intercritically reheated coarse-grained zone (IRCGHAZ), supercritically reheated coarse-grained zone (SRCGHAZ)) of the subject steel plate were simulated employing a Gleeble 3 800 thermomechanical simulator. The microstructure of the CGHAZ consists of lathlike bainite (LB) under E less than 50 kJ/cm. The microstructure changes gradually into granular bainite (GB) associated with coarsened martensite/austenite (M/A) constituents in the cases of E greater than 100 kJ/cm. Ductile impact fracture behavior is observed under the CGHAZ conditions with E less than 100 kJ/cm, while brittle fracture is rendered with E greater than 100 kJ/cm. The IRCGHAZ is the so called local brittle zone (LBZ) under all the tested conditions. This is attributed to the formation of coarse M/A constituents. The SRCGHAZs with moderate and small E which is no greater than 50 kJ/cm show ductile fracture. These are LBZs with increased E which is once again attributed to the formation of GB. The increase of T_P^2 leads to improved impact toughness in the SRCGHAZ. This is attributed to increased hardenability of austenite resulting in transformed-microstructure consisting of fine LB and GB.

Key words: weathering plate steel for bridge; simulated heat affected zones; impact toughness

Effect of welding polar on dry hyperbaric GMAW process LI Kai, GAO Hongming, LI Haichao, DING Yang (State Key Laboratory of Advanced Welding and Joining, Harbin Institute of Technology, Harbin 150001, China). pp 108 – 112

Abstract: Dry hyperbaric gas metal arc welding (GMAW) experiments with direct current electrode positive (DCEP) and direct current electrode negative (DCEN) were carried out. The process characteristics with different welding polar were studied at ambient pressure 0.1 – 2.0 MPa. By using DCEP, welding spatters appears when the pressure reached 0.2 MPa. Spatter generation level increases and spatter size decreases with increasing pressure. When ambient pressure is more than 0.4 MPa, welding process of DCEN is stable with nearly no spatter generation. The characteristics of two spatter types in DCEP were analyzed by high speed camera. The droplet deviated spatter is generated in the process of droplet repelled transfer. Another type of droplet rebounded spatter, is generated by the electromagnetic force. The reason of few spatters generating with DCEN was discwssed.

Key words: dry hyperbaric welding; gas metal arc welding; weld appearance; spatter